OXFORD

Cerebral Cortex, 2016, 1–11

doi: 10.1093/cercor/bhw109
Original Article

ORIGINAL ARTICLE

Developmental Changes in Topological Asymmetry Between Hemispheric Brain White Matter Networks from Adolescence to Young Adulthood

Suyu Zhong, Yong He, Hua Shu and Gaolang Gong

State Key Laboratory of Cognitive Neuroscience and Learning & IDG/McGovern Institute for Brain Research, Beijing Normal University, Beijing, China

Address correspondence to Gaolang Gong, PhD, State Key Laboratory of Cognitive Neuroscience and Learning & IDG/McGovern Institute for Brain Research, Beijing Normal University, Beijing 100875, China. Email: gaolang.gong@bnu.edu.cn

Abstract

Human brain asymmetries have been well described. Intriguingly, a number of asymmetries in brain phenotypes have been shown to change throughout the lifespan. Recent studies have revealed topological asymmetries between hemispheric white matter networks in the human brain. However, it remains unknown whether and how these topological asymmetries evolve from adolescence to young adulthood, a critical period that constitutes the second peak of human brain and cognitive development. To address this question, the present study included a large cohort of healthy adolescents and young adults. Diffusion and structural magnetic resonance imaging were acquired to construct hemispheric white matter networks, and graph-theory was applied to quantify topological parameters of the hemispheric networks. In both adolescents and young adults, rightward asymmetry in both global and local network efficiencies was consistently observed between the 2 hemispheres, but the degree of the asymmetry was significantly decreased in young adults. At the nodal level, the young adults exhibited less rightward asymmetry of nodal efficiency mainly around the parasylvian area, posterior tempo-parietal cortex, and fusiform gyrus. These developmental patterns of network asymmetry provide novel insight into the human brain structural development from adolescence to young adulthood and also likely relate to the maturation of language and social cognition that takes place during this period.

Key words: connectome, development, diffusion MRI, graph theory, lateralization

Introduction

The human brain is structurally and functionally asymmetrical, or lateralized (Toga and Thompson 2003). In healthy individuals, a number of brain phenotypes have been shown to exhibit asymmetry, including gray matter (GM) volume (Beaton 1997; Good et al. 2001), cortical thickness (Luders et al. 2006), white matter (WM) integrity (Buchel et al. 2004; Catani et al. 2007; Qiu et al. 2011; Thiebaut de Schotten, Dell'Acqua, et al. 2011), and functional activation (Springer et al. 1999; Devlin et al. 2003). These asymmetries are putatively associated with the functional specialization of language, motor, or other cognitive functions (Toga and Thompson 2003). Importantly, various psychiatric and neurological diseases exhibit significant alterations of hemispheric brain asymmetries; these changes provide valuable insight into the underlying pathological mechanisms and also suggest the possibility of asymmetry-based biomarkers for these diseases (Bilder et al. 1999; Herbert et al. 2002; Leonard and Eckert 2008; Shaw et al. 2009).

Notably, hemispheric asymmetries in the human brain continually change throughout the lifespan. A number of studies have demonstrated developmental changes in the hemispheric asymmetry of measures of both brain structure and function, including cortical thickness (Zhou et al. 2013), WM properties (Gong, Jiang, Zhu, Zang, He, et al. 2005; Gong, Jiang, Zhu, Zang,

Wang, et al. 2005; Lebel and Beaulieu 2009; Thiebaut de Schotten, Ffytche, et al. 2011; Song et al. 2015), functional activation (Cabeza 2002), homotopic resting-state functional coupling (Zuo et al. 2010), and resting-state network organization (Agcaoglu et al. 2015). These developmental changes in brain asymmetries might underlie the maturation of or decline in the specialization of specific human cognitive functions (Zhou et al. 2013). Intriguingly, developmental changes in human brain asymmetries might be modulated by gender. For instance, the leftward asymmetry of the local surface area around the paracentral lobule emerged at birth in boys but 2 years after birth in girls (Li, Nie, et al. 2014).

In recent years, diffusion magnetic resonance imaging (MRI) techniques have been applied to virtually reconstruct WM tracts and to model the human brain as a complex network/graph (Le Bihan 2003; Bullmore and Sporns 2009). Graph theoretical approaches provide a powerful tool to examine the topological organization of the constructed human brain WM networks. These WM networks have been shown to exhibit a number of nontrivial topological properties, for example, small-world organizational principles (Iturria-Medina et al. 2007; Gong, He, et al. 2009), central communication hubs and highway connections (Hagmann et al. 2008; Gong, He, et al. 2009; Li et al. 2013), modular structure (Hagmann et al. 2008, 2010; Yap et al. 2011), and rich-club architecture (van den Heuvel and Sporns 2011; van den Heuvel et al. 2012; van den Heuvel et al. 2013). The topology of the entire human brain network also evolves across the lifespan (Gong, Rosa-Neto, et al. 2009; Hagmann et al. 2010; Yap et al. 2011).

By studying WM networks within a hemisphere, several studies have demonstrated significant topological asymmetry between hemispheric WM networks. For instance, in healthy adults, the right hemispheric network exhibited more efficient WM connections and a greater degree of small-worldness compared with the left (Iturria-Medina et al. 2011; Li, Chen, et al. 2014). In contrast, the neonatal brain showed greater network efficiency in the left hemisphere compared with the right (Ratnarajah et al. 2013). These contrasting findings suggest that development affects the topological asymmetry of the networks in the 2 hemispheres. In line with this hypothesis, Caeyenberghs and Leemans (2014) reported a significant change in the degree of asymmetry of the global network efficiency from young-to-old adulthood (i.e., 20–86 years).

However, it has remained unknown whether and how the asymmetry of network topology evolves from adolescence to young adulthood, a critical period that constitutes the second peak of human brain and cognitive development (Paus 1999; Sowell et al. 1999; Blakemore 2008). During this period, substantial neuronal changes (e.g., the elimination of synaptic spines, turnover of synaptic circuitry, dendritic growth, and axonal myelination) have been observed (Rakic et al. 1994; Petanjek et al. 2008, 2011), supporting a protracted brain network maturation at the macro scale. Given the differences in hemispheric asymmetries that have been previously observed between adolescence and young adulthood (e.g., cortical thickness and WM integrity), we hypothesized the existence of dramatic differences in the topological asymmetry of hemispheric networks. Such differences in asymmetry might serve as structural substrates for the specific types of cognitive development that take place during this period. To test this hypothesis, we used diffusion MRI to construct hemispheric WM networks in a relatively large cohort of healthy adolescents and young adults and then applied graph theoretical approaches to quantify multiple topological parameters for the hemispheric networks.

Materials and Methods

Participants

There were 106 adolescents (age range, 11.0~15.9 years; mean 13.6 ± 1.16 years; female/male: 49/57) and 98 young adults (age range, 21.0~25.9 years; mean 23.1 ± 1.30 years; female/male: 52/46) in our cohort. No gender difference was observed between the 2 groups (2-tailed Pearson χ^2 test, $P = 0.33$). All participants were Han Chinese and were recruited through the parent network and by local advertisements on campus. The vast majority of participants are right-handed, and only 3 adolescents are left-handed. All participants had no history of neurological or psychiatric disorders. Written informed consent was obtained from each of the participants or their guardians. The protocol was approved by the Institutional Review Board (IRB) of the State Key Laboratory of Cognitive Neuroscience and Learning at Beijing Normal University.

MRI data Acquisition

All MRI scans were performed on the same 3 T Siemens Tim Trio MRI scanner at the Imaging Center for Brain Research, Beijing Normal University. T1-weighted images were acquired using a magnetization prepared rapid gradient echo (MPRAGE) sequence with the following imaging parameters: repetition time (TR) = 2530 ms; echo time (TE) = 3.39 ms; inversion time (TI) = 1100 ms; slice thickness = 1.33 mm; flip angle = 7°; no interslice gap; 144 sagittal slices covering the whole brain; matrix size = 256 × 256; and field of view (FOV) = 256 × 256 mm^2. For the diffusion-weighted imaging (DWI) scans, a single-shot, twice-refocused spin-echo diffusion echo-planar imaging (EPI) sequence was applied with the following parameters: TR = 8,000 ms; TE = 89 ms; 30 optimal diffusion-weighted directions with a *b*-value of 1000 s/mm^2 and one image with a *b*-value of 0 s/mm^2; data matrix = 128 × 128; FOV = 282 × 282 mm^2; slice thickness = 2.2 mm; 62 axial slices with no interslice gap; voxel size = 2.2 × 2.2 × 2.2 mm^3; and number of averages = 2.

Hemispheric Brain WM Network Construction

The processing of all DWI images was performed using a pipeline tool of diffusion MRI, that is, PANDA (Cui et al. 2013). The processing included brain extraction, correction for eddy current distortion and simple head motion, *b*-matrix correction (Leemans and Jones 2009), and computations for diffusion tensor and fractional anisotropy (FA). To study the topological asymmetry of human brain networks, we constructed the 2 hemispheric brain WM networks for each subject. The network construction flowchart is illustrated in Figure 1, and the technical details are described below.

Node Definition for the Hemispheric WM Networks

To construct a brain network, 2 basic network elements must be determined: nodes and edges. For each hemisphere, the entire GM was parcellated into 512 uniform regions of interest (ROIs) using a random partition procedure (Zalesky et al. 2010); each ROI represented a node of the hemispheric network. First, the AAL template in Montreal Neurological Institute (MNI) space was binarized, excluding the cerebellum. The resultant mask and its flipped version were combined to yield a symmetric mask for the entire cerebral cortex. The random parcellation procedure was then applied within the right side of the symmetric mask. Next, the resultant 512-ROI set for the right side was flipped into the left hemisphere. This flipping ensured one-to-one correspondence of ROIs/nodes between the left and right

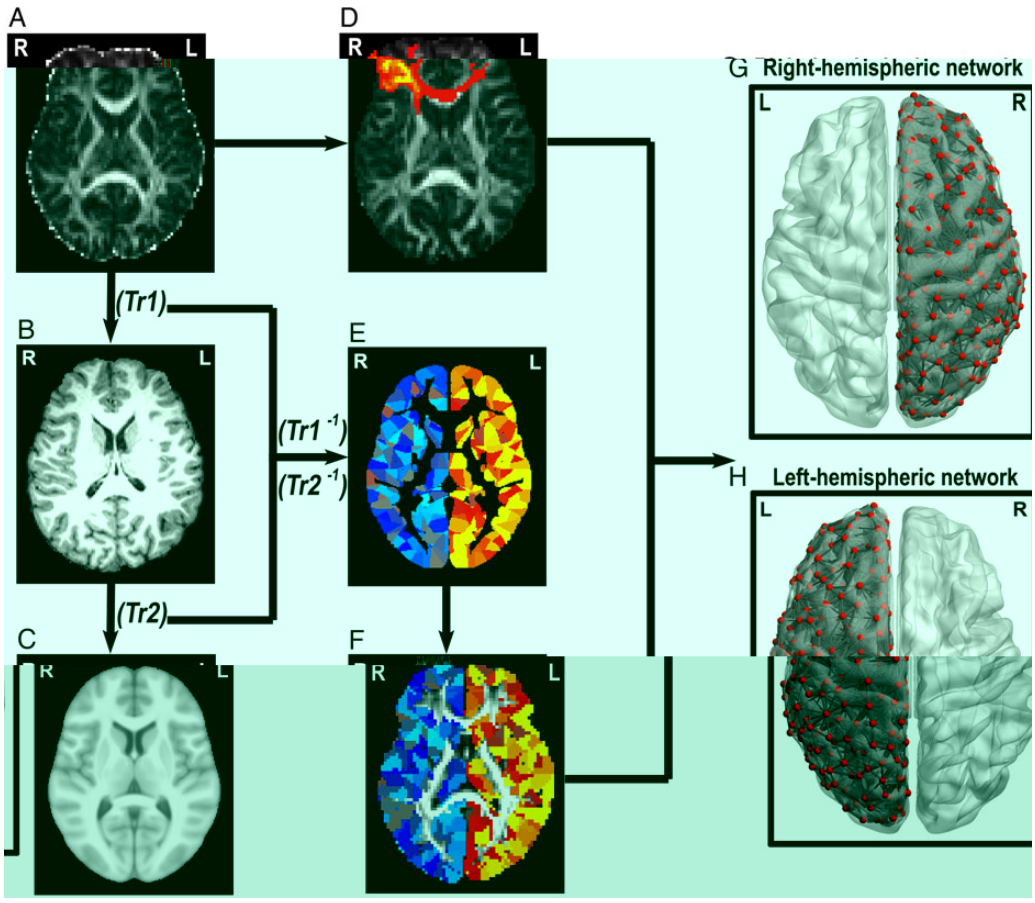

Figure 1. Flowchart for of the procedure used to construct the 2 hemispheric brain WM networks. (*A*) individual FA image; (*B*) individual T1-weighted image; (*C*) symmetric ICBM-152 T1 template; (*D*) diffusion MRI probabilistic tractography; (*E*) hemispheric parcellation atlas in the MNI space; (*F*) native-space hemispheric parcellation; (*G*) 3D rendering of the right hemispheric brain network in the MNI space, as generated by BrainNet viewer (Xia et al. 2013). Each node is represented by a red ball; (*H*) 3D rendering of the left hemispheric brain network. Tr1: the transformation from diffusion MRI native space (*A*) to the T1-weighted image (*B*). Tr2: the transformation from the T1-weighted image (*B*) to the symmetric ICBM-152 T1 template in MNI space (*C*). $Tr1^{-1}$ and $Tr2^{-1}$ denote the inverse transformation of Tr1 and Tr2, respectively. L: left; R: right.

hemispheric networks, enabling direct comparisons between the 2 hemispheric networks. For each subject, the ROIs set in MNI space were further transformed into the native diffusion space, as proposed previously (Gong, He, et al. 2009). Briefly, the individual FA images were first coregistered to the T1-weighted images. The T1-weighted images were then nonlinearly normalized to the symmetric ICBM-152 T1 template in MNI space using FMRIB's Nonlinear Image Registration Tool (FNIRT, http://www.fmrib.ox.ac.uk/fsl/). Finally, the inverse transformations were applied to the parcellation of the MNI space, resulting in native-space GM parcellations for each subject. The transformation procedures were also implemented using PANDA.

Edge Definition for the Hemispheric WM Networks

Probabilistic tractography in FSL was used to define network edges (Gong, Rosa-Neto, et al. 2009; Li et al. 2012). Specifically, Markov Chain Monte Carlo sampling was first applied to estimate voxel-wise probability density functions (PDFs). A 2-fiber model was used for each voxel. Each node was then selected as a seed region, and the probabilistic tractography was conducted by sampling 5000 tracts for each voxel within the seed region. For each sample, the principal diffusion direction was determined from the local PDF. The tract was then traced 0.5 mm along the principal direction to a new location. This process continued until it reached the boundary of brain mask, or the path loops back to itself, or the turning angle was >60°. The connectivity probability from region *i* to region *j* was defined as the edge weight after distance was corrected for (Chu et al. 2015). Notably, the estimated connectivity probability from *i* to *j* is not necessarily equivalent to the probability from *j* to *i* because probabilistic tractography depends on the seeding location. Here, we simply averaged the 2 connectivity probabilities as the final edge weight between *i* and *j*. Because hemispheric networks were our main focus, the seed and target regions were confined to the same hemisphere. For each subject, the analysis yielded two 512 × 512 symmetric weighted matrices, each representing a hemispheric network of the human brain.

Network Parameters

Network measures were calculated using the Gretna package (Wang et al. 2015). In graph theory, topological network efficiencies have been widely used to characterize the capacity of parallel information processing within a complex network (Latora and Marchiori 2001, 2003). In particular, these measures are conceptually preferable for analyses of brain network topology (Achard and Bullmore 2007). We therefore focused on efficiency-related parameters when assessing the asymmetry of hemispheric

brain networks. Specifically, nodal efficiency, global network efficiency, and local network efficiency were computed. The definitions for these parameters are described below.

Nodal Efficiency

Nodal efficiency (E_{nodal}) represents the capacity of a node to communicate with the other nodes of a network and is defined as follows

$$E^G_{nodal}(i) = \frac{1}{N-1}\sum_{i\neq j\in G}\frac{1}{L_{ij}},$$

where L_{ij} is the shortest path length between node i and node j and represents the distance between node i and node j; and N denotes the number of nodes of the network G.

Network Global Efficiency

Global efficiency is a global measure of the information transferring ability of the entire network and is computed as the mean of the nodal efficiencies of all of the nodes of the network (Latora and Marchiori 2001):

$$E^G_{glob} = \frac{1}{N(N-1)}\sum_{i\in G}\sum_{j\neq i\in G}\frac{1}{L_{ij}}$$

Local Network Efficiency

Local efficiency corresponds to the average efficiency of information flow within the local environment and reflects the average ability of a network to tolerate faults (Latora and Marchiori 2001). The local efficiency of a network is computed as follows

$$E^G_{loc} = \frac{1}{N}\sum_{i\in G}E^{G_i}_{glob},$$

where G_i is the subgraph composed of the nearest neighbors of node i and the connections among them.

Asymmetry Index

To quantify the degree of asymmetry, a commonly used asymmetry index (AI) was calculated using the following formula

$$AI = \frac{M_L - M_R}{M_L + M_R}$$

For network efficiencies, M_L and M_R represent the global or local efficiency of the entire left and right hemispheric network, respectively. For nodal efficiencies, M_L and M_R represent the nodal efficiency of corresponding ROIs from the left and right hemispheric networks, respectively. In total, 512 values of AI were obtained for nodal efficiency, one for each node. Notably, here, a positive value of AI represents a leftward asymmetry, while a negative value of AI represents a rightward asymmetry.

Statistical Analysis

For each group (i.e., adolescents and young adults), we first tested for significant within-group asymmetries in global efficiency, local efficiency, or nodal efficiency. Specifically, we applied a linear model with repeated measures, in which the hemisphere was taken as the repeated variable (i.e., left and right as the repeated measure) and gender was used as a covariate. The "gender × hemisphere" interaction was evaluated first, but this interaction was not significant for any of the efficiency parameters, and therefore this interaction term was excluded in the final model. Given the previously reported association of network efficiency and brain size (Yan et al. 2011) as well as the reports of between-hemisphere differences in hemispheric size (Giedd et al. 1999), the intracranial volume (ICV) of the hemispheres was included as a covariate in the statistical model. Here, the hemispheric ICV was computed by summing the volume of WM, GM, and cerebrospinal fluid within each hemisphere. The tissue segmentation was applied to the T1-weighted images, and the procedure was implemented using SPM8 (http://www.fil.ion.ucl.ac.uk/spm/software/spm8/).

For network efficiencies, $P < 0.05$ was considered significant. For nodal efficiencies (512 in total), the false discovery rate (FDR) procedure was applied to correct for multiple comparisons (Genovese et al. 2002), and $q < 0.05$ was considered significant.

Next, we assessed age-related effects on the AI of the network's global efficiency, local efficiency, and nodal efficiencies. For each AI measure, the "group × gender" interaction was first evaluated. If the interaction was not significant, the interaction term was excluded in the statistical model. The main group effects were then evaluated after controlling for gender, whole-brain ICV, and the difference in hemispheric ICV. For the AI of nodal efficiency (512 in total), the statistical procedure was confined to the nodes/ROIs that showed a significant asymmetry in at least one of the groups, and $q < 0.05$ after FDR correction was considered significant.

Validation

Here, a random parcellation procedure was used to define network nodes. To evaluate the influence of the parcellation scheme on our results, we repeated the random parcellation within the 2 hemispheres using the exact same procedure above and constructed hemispheric brain networks. To distinguish the 2 random parcellation schemes, we referred to the original as parcellation I and to the one used for validation as parcellation II. All of the network topological asymmetry analyses were reapplied using the hemispheric networks of the parcellation II.

Results

Within-group Asymmetry of Local and Global Network Efficiencies

The within-group asymmetries in global and local network efficiencies for both groups are illustrated in Figure 2. Significant

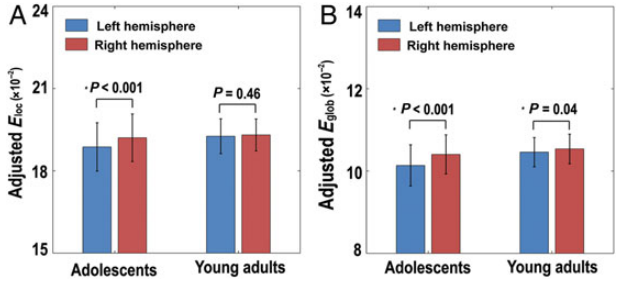

Figure 2. Within-group asymmetry of the local and global efficiency of the hemispheric networks. (A) Local efficiency (E_{loc}); (B) Global efficiency (E_{glob}). For each group, the statistical analysis was conducted after the data were adjusted for hemispheric ICV and gender.

rightward (i.e., right > left) hemispheric asymmetry in local network efficiency was observed in the adolescents ($t = -5.32$, $P < 0.001$) but not in the young adults ($t = -0.74$, $P = 0.46$). Significant rightward asymmetry in global network efficiency was observed in both groups (adolescents: $t = -7.28$, $P < 0.001$; young adults: $t = -2.11$, $P = 0.03$).

Between-group Differences in the Asymmetry of Local and Global Network Efficiency

There was no significant "group × gender" interaction for the AI of local and global network efficiency. A significant group main effect was observed for the AI of both local efficiency ($t = -3.08$; $P < 0.001$) and global efficiency ($t = -3.71$; $P < 0.001$), as shown in Table 1 and Figure 3. Specifically, compared with the adolescents, the young adults exhibited decreased rightward asymmetry in both local and global efficiency. Post hoc analysis revealed a significant increase or trend toward an increase in network efficiency in both hemispheres from adolescence to young adulthood (Fig. 3). Nevertheless, the degree of increase for the left hemisphere (E_{loc}: $t = -3.29$; $P = 0.0012$; E_{glob}: $t = -4.981$; $P < 0.001$) was greater than that for the right (E_{loc}: $t = -1.08$; $P = 0.28$; E_{glob}: $t = -2.17$; $P = 0.03$), ultimately leading to decreased rightward asymmetry in the young adults.

Within-group Asymmetry of Nodal Efficiency

For each group, the map of mean nodal efficiency within each hemisphere is illustrated in Figure 4A. Visual inspection suggests that the spatial patterns of mean nodal efficiency of the 2 hemispheres were highly similar. In both groups, quantitative linear correlational analysis across all nodes revealed very high correlation coefficients between the 2 hemispheres (Fig. 4B, $R > 0.99$, $P < 0.0001$). Notably, a paired t-test of the mean nodal efficiency (512 nodes in total) between the 2 hemispheres showed that in both groups, the mean nodal efficiency of the right hemisphere was significantly higher (adolescents: $t = -28.85$, $P < 0.0001$; young adults: $t = -8.37$, $P < 0.0001$), indicating a rightward asymmetry of mean nodal efficiency on average.

The between-hemisphere difference in mean nodal efficiency for each group is illustrated in Figure 4C. The hemispheric network nodes that showed significant between-hemisphere differences in nodal efficiency (FDR-corrected $P < 0.05$) in each group were projected onto the cortical surface, as demonstrated in Figure 4D. In both groups, the majority of nodal efficiency asymmetries were rightward, but the proportion differed. Specifically, 61.5% of nodes exhibited rightward asymmetry in the adolescents but only 21.3% exhibited rightward asymmetry in the young adults. The proportion of leftward asymmetric nodes was 0.59 and 7.62% in the adolescents and young adults, respectively. In the adolescents, the network nodes that exhibited rightward asymmetry in nodal efficiency covered a wide range of regions, including the postcentral gyrus, inferior parietal, precuneus, superior parietal gyrus, angular gyrus, and supramarginal gyrus of the parietal lobe; the middle temporal gyrus, inferior temporal gyrus, superior temporal gyrus, and fusiform gyrus of the temporal lobe; the precentral gyrus, superior medial frontal gyrus, and middle frontal gyrus of the frontal lobe; the middle occipital gyrus of the occipital lobe; the anterior and median cingulate and the paracingulate gyri of the limbic cortex; and the insula. In the young adults, the rightward asymmetric nodes were located in similar regions but covered a smaller area (Fig. 4D). In contrast, the leftward asymmetric nodes were mainly located around the supplementary motor area, fusiform gyrus, middle occipital gyrus, inferior temporal gyrus, lingual gyrus, calcarine fissure and surrounding cortex, middle temporal gyrus, dorsolateral superior frontal gyrus, and superior and inferior occipital gyrus.

Between-group Differences in the Asymmetry of Nodal Efficiency

After FDR correction, no significant "group × gender" interaction effect was observed for the AI of nodal efficiency for any node. The significant group difference in the AI of nodal efficiency is illustrated in Figure 5A. As shown, the network nodes that exhibited such a group difference were predominately located around

Table 1 Statistical results for the local and global network efficiencies using the 2 parcellation schemes

	Node parcellation I		Node parcellation II	
	t-value	*P*-value	*t*-value	*P*-value
Within-group asymmetry of E_{loc}				
Adolescents	−5.32[a]	0.00	−5.59[a]	0.00
Young adults	−0.74[a]	0.46	−2.71[a]	0.00
Within-group asymmetry of E_{glob}				
Adolescents	−7.28[a]	0.00	−6.17[a]	0.00
Young adults	−2.11[a]	0.03	−2.43[a]	0.02
Group comparison of the AI				
AI of E_{loc}	−3.08[b]	0.00	−2.60[b]	0.01
AI of E_{glob}	−3.71[b]	0.00	−2.88[b]	0.00

E_{loc}, local efficiency; E_{glob}, global efficiency; AI, asymmetry index.
[a]Negative values represent rightward asymmetry.
[b]Negative values represent a decrease in rightward asymmetry.

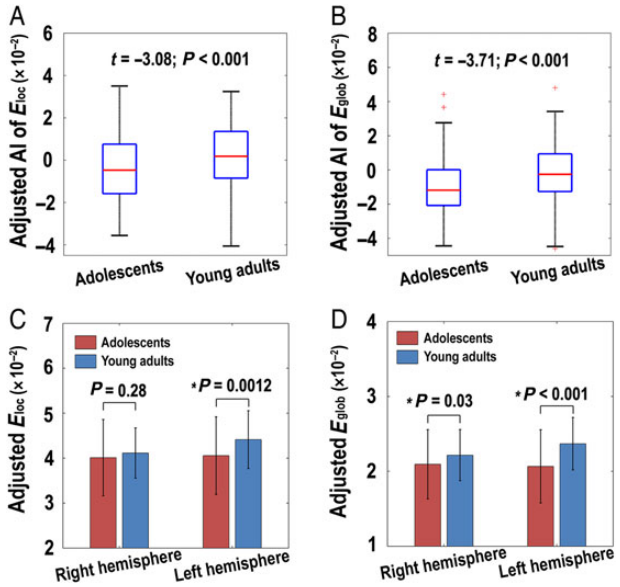

Figure 3. Between-group differences in the AI of the local and global efficiency of the hemispheric networks. The box plots depict local (*A*) and global efficiency (*B*). Before conducting the group comparisons, the data were adjusted for whole-brain ICV, hemispheric ICV difference, and gender. (*C*) Bar charts depicting group differences in the local efficiency of each hemisphere. (*D*) Bar charts depicting group differences in the global efficiency. Before conducting the group comparisons for each hemisphere, the hemisphere ICV and gender were adjusted.

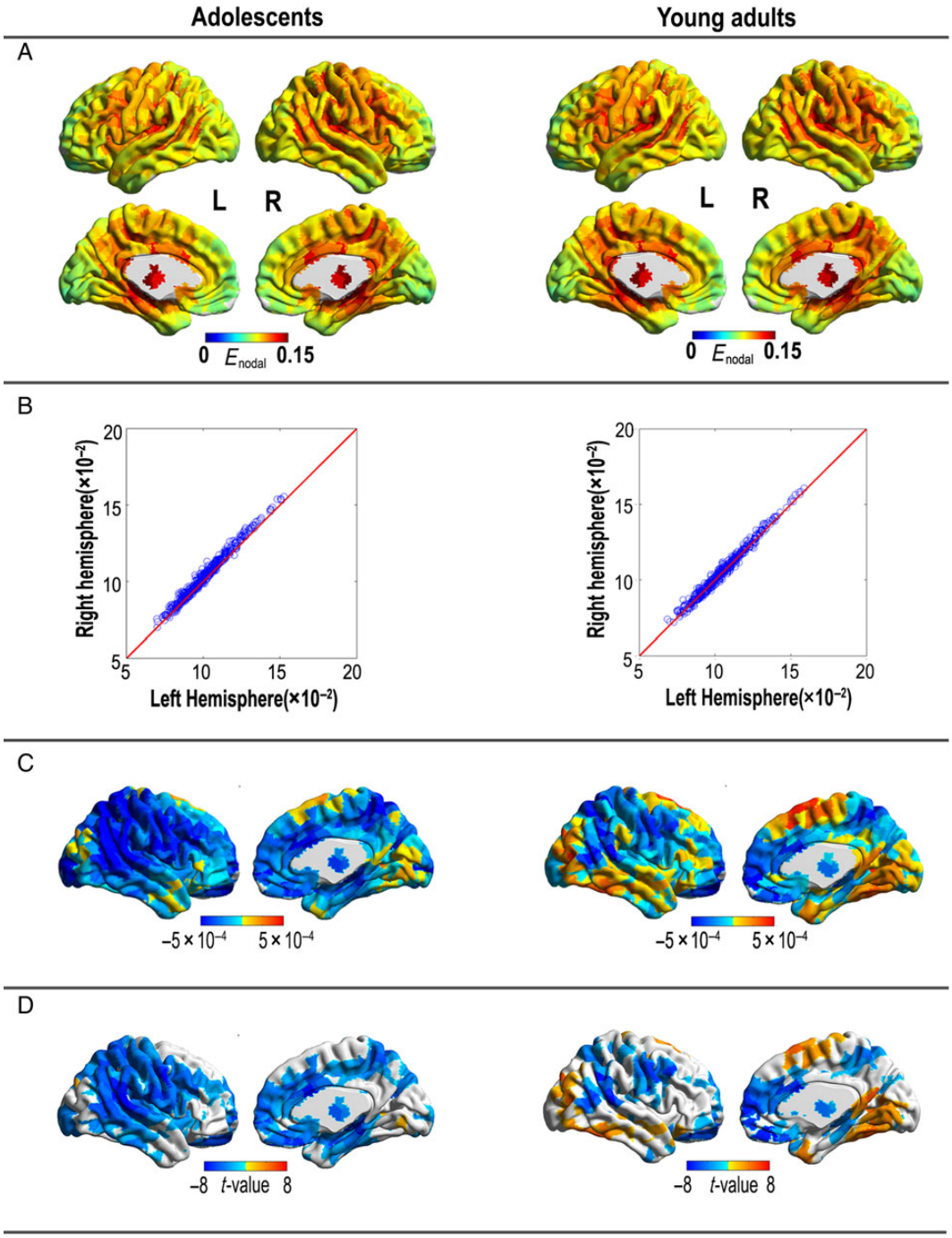

Figure 4. Within-group asymmetry in nodal efficiency across the brain. The nodal values were projected onto the cortical surface. (*A*) Surface map of mean nodal efficiency for the 2 hemispheric networks. Color represents the mean nodal efficiency across all of the subjects in each group. (*B*) The between-hemisphere correlation of mean nodal efficiency across all nodes (512 in total). Each blue circle represents a ROI per node. (*C*) Surface map of the difference in mean nodal efficiency (left–right) for each group. Color represents the value of the difference in mean nodal efficiency between the left and right hemisphere. (*D*) Surface map of statistically significant nodal efficiency asymmetry for both groups. Color represents the *t*-values. Positive and negative *t*-values represent leftward and rightward asymmetry, respectively. L, left hemisphere; R, right hemisphere. E_{nodal}, mean nodal efficiency.

the posterior temporal cortex (i.e., the posterior middle temporal gyrus, posterior inferior temporal gyrus and posterior superior temporal gyrus), supramarginal gyrus, fusiform gyrus, rolandic operculum, and inferior parietal cortex (Table 2). Overall, these nodes showed less rightward asymmetry in the young adults compared with the adolescents.

Validation with Another Parcellation Scheme

For both global and local network efficiencies, the statistical results for parcellation II were highly consistent with those for parcellation I (Table 1). In each group, the nodal efficiency asymmetry maps that were based on parcellation II were largely

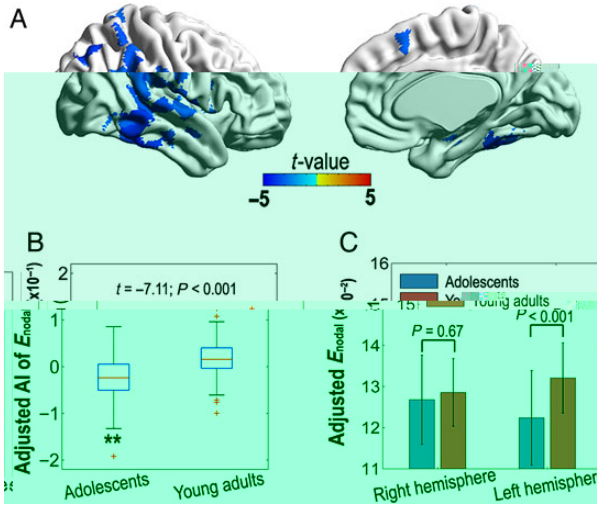

Figure 5. Between-group differences in the AI of nodal efficiency. The nodal values were projected onto the cortical surface. (*A*) Cortical surface showing network nodes with significant group differences (FDR-corrected $P < 0.05$). Color represents the *t*-values. Negative *t*-values indicate a decrease in rightward asymmetry from adolescence to young adulthood. (*B*) Box plot of group differences in the AI, based on the mean AI of observed significant nodes. The data were adjusted for whole-brain ICV, hemispheric ICV differences, and gender. (*C*) Bar charts depicting group differences in the mean local efficiency in each hemisphere. The data were adjusted for hemispheric ICV and gender. **Significant asymmetry ($P < 0.05$).

compatible with those based on parcellation I. Significant correlations between the *t*-value maps for the 2 parcellations were observed across voxels (adolescents: $r = 0.849$, $P < 0.001$; young adults: $r = 0.697$, $P < 0.001$). Furthermore, the *t*-values of the group differences in the AI of nodal efficiency were also highly correlated between the 2 parcellations ($r = 0.54$, $P < 0.001$). These consistent results between the 2 parcellation schemes demonstrate the robustness of our findings.

Finally, to evaluate the effects of left-handedness on above results, we reran all analyses after controlling for the handedness factor in the statistical model, or simply excluding the 3 left-handed subjects in our analysis. Both results are highly consistent with our current findings (data not shown).

Discussion

Using a large cohort of samples, we investigated developmental effects on topological asymmetries of the human brain WM networks from adolescence to young adulthood. In both adolescents and young adults, rightward asymmetries in network efficiency were consistently observed between the 2 hemispheres, but the degree of asymmetry was reduced in the young adults. Locally, the degree of rightward asymmetry in nodal efficiency was reduced primarily around the parasylvian area, posterior temporal-parietal cortex, and fusiform gyrus. These findings provide direct evidence of changes in network asymmetry from adolescence to young adulthood; these changes likely underlie the rapid development of language and social cognition that takes place during this period.

The Right Hemispheric Network is More Efficient in Adolescents and Young Adults

The topological organization of human WM networks has been demonstrated to be asymmetric. For example, Iturria-Medina et al. (2011) provided the first demonstration of a rightward topological asymmetry of large-scale WM networks in healthy adults. Along this line, Caeyenberghs and Leemans (2014) and Ratnarajah et al. (2013) studied healthy elderly and newborn populations, respectively, and also revealed asymmetrical patterns in hemispheric network topologies during those developmental stages. Our data went one step further and revealed a rightward asymmetry of network efficiency in both adolescents (age range: 11.0–15.9 years) and young adults (age range: 21.0–25.9 years). Taken together, these results suggest that asymmetry in network topology exists through different developmental stages across the lifespan. Given that both general (i.e., IQ) and specific cognitive/behavioral abilities (i.e., visuospatial and executive function performance) have been shown to be associated with the whole-brain network efficiencies of WM networks (Li et al. 2009; Wen et al. 2011), the observed asymmetry in hemispheric network efficiencies is likely related to hemisphere-specific functional/behavioral specializations.

The observed rightward asymmetry in network efficiency suggests that the right hemisphere is intra-connected in a better integrated way, allowing for more efficient communication at the hemispheric level. Notably, there has been a longstanding notion argument that the right hemisphere is more important for global or parallel processing than the left (Delis et al. 1986), suggesting the presence of rightward structural/functional asymmetry in within-hemispheric organization. The currently observed network efficiency asymmetry provides further support for this hypothesis. Consistently, rightward asymmetry in network efficiency has been previously reported in 11 healthy adults

Table 2 The percentage of voxels in AAL regions that exhibited a significant group difference in nodal efficiency asymmetry

AAL region	Percentage	Type
Middle temporal gyrus	18.34	Association
Inferior temporal gyrus	17.13	Association
Superior temporal gyrus	14.80	Association
Supramarginal gyrus	8.18	Association
Fusiform gyrus	7.53	Association
Rolandic operculum	5.20	Association
Inferior parietal, but supramarginal and angular gyri	5.00	Association
Angular gyrus	3.96	Association
Postcentral gyrus	3.38	Primary
Insula	3.35	Paralimbic
Superior parietal gyrus	1.97	Association
Supplementary motor area	1.71	Association
Inferior frontal gyrus, opercular part	1.69	Association
Middle occipital gyrus	1.63	Association
Hippocampus	1.53	Limbic
Heschl gyrus	1.26	Primary
Superior occipital gyrus	0.87	Association
Inferior occipital gyrus	0.60	Association
Parahippocampal gyrus	0.58	Paralimbic
Precentral gyrus'	0.47	Primary
Temporal pole: superior temporal gyrus	0.34	Paralimbic
Median cingulate and paracingulate gyri	0.19	Paralimbic
Precuneus	0.15	Association
Lenticular nucleus, putamen	0.07	Subcortical
Amygdala	0.04	Subcortical
Cuneus	0.03	Association
Temporal pole: middle temporal gyrus	0.01	Paralimbic
Inferior frontal gyrus, triangular part	0.00	Association
Paracentral lobule	0.00	Association

(Iturria-Medina et al. 2011). Notably, rightward asymmetry in global efficiency was also found in macaque monkeys (Iturria-Medina et al. 2011). Therefore, it is likely that these observed network asymmetries were, at least partly, inherited from our ancestors (Ocklenburg and Gunturkun 2012).

However, conflicting results have been reported. For example, Caeyenberghs and Leemans (2014) reported leftward asymmetry in network efficiencies. It should be noted that there were substantial between-study differences in hemispheric WM network construction methods (e.g., network resolution and tractography methods). For example, the hemispheric network had a lower resolution in Caeyenberghs and Leemans 2014: 90 nodes (low resolution) versus 512 nodes in the present study (high resolution). The WM tractography algorithm and weighting strategy for network edges also differed: a deterministic tractography was used by Caeyenberghs and Leemans, but we applied a probabilistic tractography in the present study. Given the fact that network construction methods can dramatically affect WM network topological properties as well as its individual differences (Zalesky et al. 2010; Bassett et al. 2011; Zhong et al. 2015), the observed contradicting results likely relate to the differences in hemispheric network resolution and tractography methods. In addition to these methodological differences, age range for the young adults is quite different, with the Caeyenberghs's group being much older (20–42 years) than ours (21–26 years). Though less likely, the WM network efficiency asymmetry may become flipped from rightward to leftward around the middle age, accounting for above conflicting results. In fact, our currently observed reduced rightward asymmetry from adolescence to young adulthood is in line with this notion. However, this possibility is essentially speculative, and life-span cohort is required to validate it in the future.

The observed asymmetry in nodal efficiency suggests that corresponding nodes in the 2 hemispheres differ in their capacity to communicate with other nodes in the same hemisphere (Bullmore and Sporns 2009). In the adolescents and young adults, the overlapping regions that exhibited rightward asymmetry in nodal efficiency were mostly located around the anterior medial and posterior lateral frontal as well as temporal-parietal junction areas. This asymmetry might relate to other structural asymmetries. For example, a rightward cortical thickness asymmetry along the lateral, mesial, and dorsal surfaces of the posterior temporal, parietal, and occipital cortices has been reported (Plessen et al. 2014). Microscopically, lower-order dendrites in the temporal-parietal junction area in the right hemisphere were longer than their counterparts in the left (Scheibel et al. 1985). Notably, in young adults, a substantial number of regions exhibited leftward asymmetry in nodal efficiency, and these regions were mainly located near medial parietal areas as well as the temporal and occipital (ventral) lobes.

Developmental Effects on the Asymmetry of Network Properties

Compared with the adolescents, the young adults exhibited significantly decreased rightward asymmetry in both local network efficiency and global network efficiency. This difference in hemispheric asymmetries is likely related to a mismatch in the developmental changes that the 2 hemispheres undergo. This hypothesis is compatible with the well-documented spatial specificity of the maturational trajectories of brain structural properties, such as GM volume (Sowell et al. 2003; Gogtay et al. 2004) and WM integrity (Imperati et al. 2011). Specifically, our data revealed a developmental

detothesp3.5i2tali70.1(sp2(deto)-203.7l.8(8k)-211.9(ef)TJ/T1(613.78030Td()Tj/T101Tf0.62740Td(ajec0(Thi)-5.3ale1948(iTJ0.6274e)-e

social brain undergoes significant functional/structural development during adolescence, leading to dramatic changes in social behaviors (Blakemore 2008). The developmental changes in nodal efficiency asymmetry that we observed likely serve as a structural substrate for the rapid development of social cognition that occurs from adolescence to young adulthood.

Notably, in the present study, there were no significant gender differences in asymmetry per se or in the developmental changes in asymmetry, suggesting that gender has a limited impact on these particular brain phenotypes. This observation is compatible with previous observations of structural cortical asymmetry (Luders et al. 2006; Zhou et al. 2013) but conflict with observations of functional network asymmetry (Tian et al. 2011). A structure–function discrepancy, however, is expected to some extent, and there is a lack of one-to-one correspondence in structural and functional connectivity (Greicius et al. 2009; Honey et al. 2009; Horn et al. 2014).

Despite the lack of gender effect on the asymmetry or its developmental changes, there was a significant gender main effect on the hemispheric network global efficiency (male greater than female), but not the local efficiency, after controlling for the hemispheric side and age group factors (see Supplementary Table 1 and Fig. 1). This observed gender effect on the hemispheric network efficiency but not on its asymmetry or developmental change is highly consistent with previous studies in hemispheric network asymmetries (Caeyenberghs and Leemans 2014), and further supports an important role of gender in human brain connectivity (Gong et al. 2011; Yan et al. 2011).

Limitations and Future Work

A few issues should be addressed. First, despite the relatively large sample size of the present study, it is still important to validate our findings by replicating our analyses in a completely independent cohort. Second, our results were based on cross-sectional analyses, and a longitudinal developmental dataset is highly desired to verify the current findings. Next, the handedness has showed an impact on network efficiency asymmetries of human brains (Li, Chen, et al. 2014). However, the present study had a very unbalanced sample size for the handedness (i.e., only 3 left-handed adolescents), and therefore it is not feasible to assess the handedness effect on network asymmetries and its developmental changes. This intriguing issue can be explored in further studies. Finally, the current study did not include cognitive/behavioral data, and the relationship between the network asymmetry changes and language/social cognitive development are essentially speculative. It would be necessary to investigate developmental changes in network asymmetry and cognitive/behavioral scores together and to explicitly evaluate the asymmetry–cognition relationships in the future.

Conclusion

The present study revealed decreased rightward asymmetry in hemispheric WM networks from adolescence to young adulthood using a large cohort. This particular developmental pattern of asymmetry provides novel insight into human brain structural development and may underlie the maturation of specific cognitive abilities that occurs during this period.

Supplementary Material

Supplementary Material can be found at http://www.cercor.oxfordjournals.org/online.

Funding

This work was supported by the 973 program (nos 2013CB837300, 2014CB846100), the National Science Foundation of China (81271649, 81322021, 31271082, 81225012, and 31221003), the 863 program (2015AA020912), and the Fundamental Research Funds for the Central Universities.

Notes

Conflict of Interest: None declared.

References

Achard S, Bullmore E. 2007. Efficiency and cost of economical brain functional networks. PLoS Comput Biol. 3:e17.

Agcaoglu O, Miller R, Mayer AR, Hugdahl K, Calhoun VD. 2015. Lateralization of resting state networks and relationship to age and gender. Neuroimage. 104:310–325.

Bassett DS, Brown JA, Deshpande V, Carlson JM, Grafton ST. 2011. Conserved and variable architecture of human white matter connectivity. Neuroimage. 54:1262–1279.

Beaton AA. 1997. The relation of planum temporale asymmetry and morphology of the corpus callosum to handedness, gender, and dyslexia: a review of the evidence. Brain Lang. 60:255–322.

Bilder RM, Wu H, Bogerts B, Ashtari M, Robinson D, Woerner M, Lieberman JA, Degreef G. 1999. Cerebral volume asymmetries in schizophrenia and mood disorders: a quantitative magnetic resonance imaging study. Int J Psychophysiol. 34:197–205.

Blakemore SJ. 2008. The social brain in adolescence. Nat Rev Neurosci. 9:267–277.

Blakemore SJ, Choudhury S. 2006. Development of the adolescent brain: implications for executive function and social cognition. J Child Psychol Psychiatry. 47:296–312.

Buchel C, Raedler T, Sommer M, Sach M, Weiller C, Koch MA. 2004. White matter asymmetry in the human brain: a diffusion tensor MRI study. Cereb Cortex. 14:945–951.

Bullmore E, Sporns O. 2009. Complex brain networks: graph theoretical analysis of structural and functional systems. Nat Rev Neurosci. 10:186–198.

Cabeza R. 2002. Hemispheric asymmetry reduction in older adults: The HAROLD model. Psychol Aging. 17:85–100.

Caeyenberghs K, Leemans A. 2014. Hemispheric lateralization of topological organization in structural brain networks. Hum Brain Mapp. 35:4944–4957.

Catani M, Allin MP, Husain M, Pugliese L, Mesulam MM, Murray RM, Jones DK. 2007. Symmetries in human brain language pathways correlate with verbal recall. Proc Natl Acad Sci U S A. 104:17163–17168.

Chu S-H, Lenglet C, Parhi KK. 2015. Joint brain connectivity estimation from diffusion and functional MRI data. Proc. SPIE 9413, Medical Imaging 2015: Image Processing; March 20; Orlando, FL, USA. 941321.

Cui Z, Zhong S, Xu P, He Y, Gong G. 2013. PANDA: a pipeline toolbox for analyzing brain diffusion images. Front Hum Neurosci. 7:42.

Delis DC, Robertson LC, Efron R. 1986. Hemispheric specialization of memory for visual hierarchical stimuli. Neuropsychologia. 24:205–214.

Dennis EL, Jahanshad N, McMahon KL, de Zubicaray GI, Martin NG, Hickie IB, Toga AW, Wright MJ, Thompson PM. 2014. Development of insula connectivity between ages 12

and 30 revealed by high angular resolution diffusion imaging. Hum Brain Mapp. 35:1790–1800.
Devlin JT, Raley J, Tunbridge E, Lanary K, Floyer-Lea A, Narain C, Cohen I, Behrens T, Jezzard P, Matthews PM, et al. 2003. Functional asymmetry for auditory processing in human primary auditory cortex. J Neurosci. 23:11516–11522.
Fu X, Giavalisco P, Liu X, Catchpole G, Fu N, Ning ZB, Guo S, Yan Z, Somel M, Paabo S, et al. 2011. Rapid metabolic evolution in human prefrontal cortex. Proc Natl Acad Sci U S A. 108: 6181–6186.
Genovese CR, Lazar NA, Nichols T. 2002. Thresholding of statistical maps in functional neuroimaging using the false discovery rate. Neuroimage. 15:870–878.
Giedd JN, Blumenthal J, Jeffries NO, Castellanos FX, Liu H, Zijdenbos A, Paus T, Evans AC, Rapoport JL. 1999. Brain development during childhood and adolescence: a longitudinal MRI study. Nat Neurosci. 2:861–863.
Gogtay N, Giedd JN, Lusk L, Hayashi KM, Greenstein D, Vaituzis AC, Nugent TF 3rd, Herman DH, Clasen LS, Toga AW, et al. 2004. Dynamic mapping of human cortical development during childhood through early adulthood. Proc Natl Acad Sci U S A. 101:8174–8179.
Gong G, He Y, Concha L, Lebel C, Gross DW, Evans AC, Beaulieu C. 2009. Mapping anatomical connectivity patterns of human cerebral cortex using in vivo diffusion tensor imaging tractography. Cereb Cortex. 19:524–536.
Gong G, He Y, Evans AC. 2011. Brain connectivity: gender makes a difference. Neuroscientist. 17:575–591.
Gong G, Jiang T, Zhu C, Zang Y, He Y, Xie S, Xiao J. 2005. Side and handedness effects on the cingulum from diffusion tensor imaging. Neuroreport. 16:1701–1705.
Gong G, Jiang T, Zhu C, Zang Y, Wang F, Xie S, Xiao J, Guo X. 2005. Asymmetry analysis of cingulum based on scale-invariant parameterization by diffusion tensor imaging. Hum Brain Mapp. 24:92–98.
Gong G, Rosa-Neto P, Carbonell F, Chen ZJ, He Y, Evans AC. 2009. Age- and gender-related differences in the cortical anatomical network. J Neurosci. 29:15684–15693.
Good CD, Johnsrude I, Ashburner J, Henson RN, Friston KJ, Frackowiak RS. 2001. Cerebral asymmetry and the effects of sex and handedness on brain structure: a voxel-based morphometric analysis of 465 normal adult human brains. Neuroimage. 14:685–700.
Greicius MD, Supekar K, Menon V, Dougherty RF. 2009. Resting-state functional connectivity reflects structural connectivity in the default mode network. Cereb Cortex. 19:72–78.
Hagmann P, Cammoun L, Gigandet X, Meuli R, Honey CJ, Wedeen VJ, Sporns O. 2008. Mapping the structural core of human cerebral cortex. PLoS Biol. 6:e159.
Hagmann P, Sporns O, Madan N, Cammoun L, Pienaar R, Wedeen VJ, Meuli R, Thiran JP, Grant PE. 2010. White matter maturation reshapes structural connectivity in the late developing human brain. Proc Natl Acad Sci U S A. 107:19067–19072.
Herbert MR, Harris GJ, Adrien KT, Ziegler DA, Makris N, Kennedy DN, Lange NT, Chabris CF, Bakardjiev A, Hodgson J, et al. 2002. Abnormal asymmetry in language association cortex in autism. Ann Neurol. 52:588–596.
Honey CJ, Sporns O, Cammoun L, Gigandet X, Thiran JP, Meuli R, Hagmann P. 2009. Predicting human resting-state functional connectivity from structural connectivity. Proc Natl Acad Sci U S A. 106:2035–2040.
Horn A, Ostwald D, Reisert M, Blankenburg F. 2014. The structural-functional connectome and the default mode network of the human brain. Neuroimage. 102(Pt 1):142–151.
Imperati D, Colcombe S, Kelly C, Di Martino A, Zhou J, Castellanos FX, Milham MP. 2011. Differential development of human brain white matter tracts. PLoS One. 6:e23437.
Iturria-Medina Y, Canales-Rodriguez EJ, Melie-Garcia L, Valdes-Hernandez PA, Martinez-Montes E, Aleman-Gomez Y, Sanchez-Bornot JM. 2007. Characterizing brain anatomical connections using diffusion weighted MRI and graph theory. Neuroimage. 36:645–660.
Iturria-Medina Y, Perez Fernandez A, Morris DM, Canales-Rodriguez EJ, Haroon HA, Garcia Penton L, Augath M, Galan Garcia L, Logothetis N, Parker GJ, et al. 2011. Brain hemispheric structural efficiency and interconnectivity rightward asymmetry in human and nonhuman primates. Cereb Cortex. 21:56–67.
Latora V, Marchiori M. 2003. Economic small-world behavior in weighted networks. Eur Phys J B Condensed Matter. 32: 249–263.
Latora V, Marchiori M. 2001. Efficient behavior of small-world networks. Phys Rev Lett. 87:198701.
Lebel C, Beaulieu C. 2009. Lateralization of the arcuate fasciculus from childhood to adulthood and its relation to cognitive abilities in children. Hum Brain Mapp. 30:3563–3573.
Le Bihan D. 2003. Looking into the functional architecture of the brain with diffusion MRI. Nat Rev Neurosci. 4:469–480.
Leemans A, Jones DK. 2009. The B-matrix must be rotated when correcting for subject motion in DTI data. Magn Reson Med. 61:1336–1349.
Leonard CM, Eckert MA. 2008. Asymmetry and dyslexia. Dev Neuropsychol. 33:663–681.
Li G, Nie J, Wang L, Shi F, Lyall AE, Lin W, Gilmore JH, Shen D. 2014. Mapping longitudinal hemispheric structural asymmetries of the human cerebral cortex from birth to 2 years of age. Cereb Cortex. 24:1289–1300.
Li L, Hu X, Preuss TM, Glasser MF, Damen FW, Qiu Y, Rilling J. 2013. Mapping putative hubs in human, chimpanzee and rhesus macaque connectomes via diffusion tractography. Neuroimage. 80:462–474.
Li L, Rilling JK, Preuss TM, Glasser MF, Damen FW, Hu X. 2012. Quantitative assessment of a framework for creating anatomical brain networks via global tractography. Neuroimage. 61:1017–1030.
Li M, Chen H, Wang J, Liu F, Long Z, Wang Y, Iturria-Medina Y, Zhang J, Yu C, Chen H. 2014. Handedness- and hemisphere-related differences in small-world brain networks: a diffusion tensor imaging tractography study. Brain Connect. 4:145–156.
Li Y, Liu Y, Li J, Qin W, Li K, Yu C, Jiang T. 2009. Brain anatomical network and intelligence. PLoS Comput Biol. 5:e1000395.
Liu X, Somel M, Tang L, Yan Z, Jiang X, Guo S, Yuan Y, He L, Oleksiak A, Zhang Y, et al. 2012. Extension of cortical synaptic development distinguishes humans from chimpanzees and macaques. Genome Res. 22:611–622.
Luders E, Narr KL, Thompson PM, Rex DE, Jancke L, Toga AW. 2006. Hemispheric asymmetries in cortical thickness. Cereb Cortex. 16:1232–1238.
Ocklenburg S, Gunturkun O. 2012. Hemispheric asymmetries: the comparative view. Front Psychol. 3:5.
Paus TSAA. 1999. Structural maturation of neural pathways in children and adolescents: in vivo study. Science. 283: 1908–1911.
Petanjek Z, Judas M, Kostovic I, Uylings HB. 2008. Lifespan alterations of basal dendritic trees of pyramidal neurons in the human prefrontal cortex: a layer-specific pattern. Cereb Cortex. 18:915–929.

Petanjek Z, Judas M, Simic G, Rasin MR, Uylings HB, Rakic P, Kostovic I. 2011. Extraordinary neoteny of synaptic spines in the human prefrontal cortex. Proc Natl Acad Sci U S A. 108:13281–13286.

Plessen KJ, Hugdahl K, Bansal R, Hao X, Peterson BS. 2014. Sex, age, and cognitive correlates of asymmetries in thickness of the cortical mantle across the life span. J Neurosci. 34:6294–6302.

Qiu D, Tan LH, Siok WT, Zhou K, Khong PL. 2011. Lateralization of the arcuate fasciculus and its differential correlation with reading ability between young learners and experienced readers: a diffusion tensor tractography study in a Chinese cohort. Hum Brain Mapp. 32:2054–2063.

Rakic P, Bourgeois J-P, Goldman-Rakic PS. 1994. Synaptic development of the cerebral cortex: implications for learning, memory, and mental illness. Prog Brain Res. 102:227–243.

Ratnarajah N, Rifkin-Graboi A, Fortier MV, Chong YS, Kwek K, Saw SM, Godfrey KM, Gluckman PD, Meaney MJ, Qiu A. 2013. Structural connectivity asymmetry in the neonatal brain. Neuroimage. 75:187–194.

Ravid D, Tolchinsky L. 2002. Developing linguistic literacy: a comprehensive model. J Child Lang. 29:417–447.

Scheibel AB, Paul LA, Fried I, Forsythe AB, Tomiyasu U, Wechsler A, Kao A, Slotnick J. 1985. Dendritic organization of the anterior speech area. Exp Neurol. 87:109–117.

Shaw P, Lalonde F, Lepage C, Rabin C, Eckstrand K, Sharp W, Greenstein D, Evans A, Giedd JN, Rapoport J. 2009. Development of cortical asymmetry in typically developing children and its disruption in attention-deficit/hyperactivity disorder. Arch Gen Psychiatry. 66:888–896.

Somel M, Franz H, Yan Z, Lorenc A, Guo S, Giger T, Kelso J, Nickel B, Dannemann M, Bahn S, et al. 2009. Transcriptional neoteny in the human brain. Proc Natl Acad Sci U S A. 106:5743–5748.

Song JW, Mitchell PD, Kolasinski J, Ellen Grant P, Galaburda AM, Takahashi E. 2015. Asymmetry of white matter pathways in developing human brains. Cereb Cortex. 25:2883–2893.

Sowell ER, Peterson BS, Thompson PM, Welcome SE, Henkenius AL, Toga AW. 2003. Mapping cortical change across the human life span. Nat Neurosci. 6:309–315.

Sowell ER, Thompson PM, Holmes CJ, Jernigan TL, Toga AW. 1999. In vivo evidence for post-adolescent brain maturation in frontal and striatal regions. Nat Neurosci. 2:859–861.

Springer JA, Binder JR, Hammeke TA, Swanson SJ, Frost JA, Bellgowan PS, Brewer CC, Perry HM, Morris GL, Mueller WM. 1999. Language dominance in neurologically normal and epilepsy subjects: a functional MRI study. Brain. 122: 2033–2046.

Thiebaut de Schotten M, Dell'Acqua F, Forkel SJ, Simmons A, Vergani F, Murphy DG, Catani M. 2011. A lateralized brain network for visuospatial attention. Nat Neurosci. 14:1245–1246.

Thiebaut de Schotten M, Ffytche DH, Bizzi A, Dell'Acqua F, Allin M, Walshe M, Murray R, Williams SC, Murphy DG, Catani M. 2011. Atlasing location, asymmetry and inter-subject variability of white matter tracts in the human brain with MR diffusion tractography. Neuroimage. 54:49–59.

Tian L, Wang J, Yan C, He Y. 2011. Hemisphere- and gender-related differences in small-world brain networks: a resting-state functional MRI study. Neuroimage. 54:191–202.

Toga AW, Thompson PM. 2003. Mapping brain asymmetry. Nat Rev Neurosci. 4:37–48.

van den Heuvel MP, Kahn RS, Goni J, Sporns O. 2012. High-cost, high-capacity backbone for global brain communication. Proc Natl Acad Sci U S A. 109:11372–11377.

van den Heuvel MP, Sporns O. 2011. Rich-club organization of the human connectome. J Neurosci. 31:15775–15786.

van den Heuvel MP, Sporns O, Collin G, Scheewe T, Mandl RC, Cahn W, Goni J, Hulshoff Pol HE, Kahn RS. 2013. Abnormal rich club organization and functional brain dynamics in schizophrenia. JAMA Psychiatry. 70:783–792.

Wang J, Wang X, Xia M, Liao X, Evans A, He Y. 2015. GRETNA: a graph theoretical network analysis toolbox for imaging connectomics. Front Hum Neurosci. 9:386.

Wen W, Zhu W, He Y, Kochan NA, Reppermund S, Slavin MJ, Brodaty H, Crawford J, Xia A, Sachdev P. 2011. Discrete neuroanatomical networks are associated with specific cognitive abilities in old age. J Neurosci. 31:1204–1212.

Xia M, Wang J, He Y. 2013. BrainNet Viewer: a network visualization tool for human brain connectomics. PLoS One. 8:e68910.

Yan C, Gong G, Wang J, Wang D, Liu D, Zhu C, Chen ZJ, Evans A, Zang Y, He Y. 2011. Sex- and brain size-related small-world structural cortical networks in young adults: a DTI tractography study. Cereb Cortex. 21:449–458.

Yap PT, Fan Y, Chen Y, Gilmore JH, Lin W, Shen D. 2011. Development trends of white matter connectivity in the first years of life. PLoS One. 6:e24678.

Zalesky A, Fornito A, Harding IH, Cocchi L, Yucel M, Pantelis C, Bullmore ET. 2010. Whole-brain anatomical networks: does the choice of nodes matter? Neuroimage. 50:970–983.

Zhong S, He Y, Gong G. 2015. Convergence and divergence across construction methods for human brain white matter networks: an assessment based on individual differences. Hum Brain Mapp. 36:1995–2013.

Zhou D, Lebel C, Evans A, Beaulieu C. 2013. Cortical thickness asymmetry from childhood to older adulthood. Neuroimage. 83:66–74.

Zuo XN, Kelly C, Di Martino A, Mennes M, Margulies DS, Bangaru S, Grzadzinski R, Evans AC, Zang YF, Castellanos FX, et al. 2010. Growing together and growing apart: regional and sex differences in the lifespan developmental trajectories of functional homotopy. J Neurosci. 30:15034–15043.